journal of the mechanical behavior of biomedical materials 133 (2022) 105347

Contents lists available at ScienceDirect

Journal of the Mechanical Behavior of Biomedical Materials

journal homepage: www.elsevier.com/locate/jmbbm

Research paper

A pilot study on active and passive ex vivo characterisation of the urinary bladder and its impact on three-dimensional modelling

Robin Trostorf [a], Enrique Morales Orcajo [a], Amelie Pötzke [a], Tobias Siebert [b], Markus Böl [a,*]

[a] Institute of Mechanics and Adaptronics, Technische Universität Braunschweig, Braunschweig D-38106, Germany
[b] Institute of Sport and Motion Science, University of Stuttgart, Stuttgart D-70569, Germany

ARTICLE INFO

Keywords:
Urinary bladder
Active characteristics
Ex vivo experiments
Whole organ
Urinary bladder modelling
Sus scrofa domesticus

ABSTRACT

Insight into the global deformation of the urinary bladder during passive and active phases is crucial for understanding the biomechanics and function of the organ. Therefore, in the present study, the three-dimensional deformations of the porcine urinary bladder were investigated using 10 cameras in ex vivo experiments. Voltages between 20 V and 40 V were applied to induce contraction without outflow (isovolumetric) and against different back pressures (isobaric). The fluid volume in the bladder and the fluid volume pushed out of the bladder in the active state were measured. During filling, a roughly constant pressure of 2.5–4 cmH_2O was measured for a large volume range, followed by a steep increase. Overall, the urinary bladder shape changes from elliptical to spherical in the active phase, resulting in a more homogeneous stress field. The active pressure decreases with increasing volume, while the actively generated stress increases up to 65 kPa at the maximum volume examined. Smaller filling volumes and lower back pressures allowed complete emptying, whereas higher back pressures prevent full emptying from larger filling states. Finally, a recently developed three-dimensional model was used to describe the active and passive bladder characteristics in order to qualitatively represent the mechanical properties. Overall, this study provides for the first time a comprehensive experimental data set at organ level that leads to an improved understanding of load transfer mechanisms within the urinary bladder and serves to validate corresponding models.

1. Introduction

As a hollow organ, the urinary bladder (UB) has two essential functions, the intermediate storage of urine (passive phase) at low pressure and the subsequent emptying (active phase). During the filling process, the healthy UB can expand to 15 times its contracted volume (Korossis et al., 2006), causing the smooth muscle tissue of the urinary bladder wall (UBW) to contract to 7 times its previously expanded length (Uvelius, 1976). The human UB stores an average of 330 to 420 ml (Blanker et al., 2001; FitzGerald et al., 2002; Latini et al., 2004), with maximum values exceeding 1000 ml (FitzGerald et al., 2002). Understanding UBW mechanics is fundamental to gain insights into healthy and diseased tissue, as millions of people suffer physical, psychological, and socioeconomic problems due to conditions such as overactive or underactive bladder dysfunction (Durden et al., 2018; Balthazar et al., 2019). Disturbances during the active phase of UB emptying can lead to urinary retention (incomplete emptying of the UB) (Andersson and Arner, 2004) and acute emergencies (Mevcha and Drake, 2010).

Anatomically, the UB is located in the pelvic cavity and is filled by a ureter from each kidney, which opens in the trigonus region at the bottom of the bladder. In the same region, the urethra is connected to allow micturition (Andersson and Arner, 2004). Microstructurally, the UBW consists of three main layers (from the inside out): The mucosal, the muscular, and the serosal layer. For a detailed description of the microstructure of the UBW, the reader is referred to Seydewitz et al. (2017), Morales-Orcajo et al. (2018) and Trostorf et al. (2021). The inner mucosal layer serves as a urinary barrier (Turner et al., 2008). Directly adjacent to the mucosal layer is the muscular layer, which consists of smooth muscle cells with different fibre directions depending on depth and location (Morales-Orcajo et al., 2018). Both layers have tension-sensitive nerves (Kanai and Andersson, 2010). Smooth muscle cells play an important role in active mechanical behaviour, while the mucosal layer generates passive stress through high stretch (Trostorf et al., 2021). The outer serosa layer surrounds the entire organ in the pelvic cavity and produces a lubricating secretion to reduce friction caused by muscle movements (Drake, 2014).

The active properties of smooth muscle differ from those of skeletal muscle in that they can actively change their length by a factor of seven, compared to four for skeletal muscle (Uvelius, 1976; Borsdorf et al., 2019). Pratusevich et al. (1995) identified the absence of sarcomeres

* Corresponding author.
E-mail address: m.boel@tu-braunschweig.de (M. Böl).

https://doi.org/10.1016/j.jmbbm.2022.105347
Received 18 March 2022; Received in revised form 5 May 2022; Accepted 26 June 2022
Available online 28 June 2022

as the factor that enables length adaptation, as it is thought to occur through a different number of contractile units in series. This effect is often referred to as plasticity (Seow et al., 2000; Seow, 2005; Tuna et al., 2012). These effects influence passive stiffness (Ratz and Speich, 2010), highlighting the importance of the reference state (Speich et al., 2009), with length adaptation occurring on a time scale of minutes to hours (Stålhand and Holzapfel, 2016).

A literature review shows that there are essentially two types of experiments for mechanical characterisation of the UBW: Tissue level experiments and organ level experiments. Passive experiments at the tissue level are described as either axial (Finkbeiner and O'Donnell, 1990; Rohrmann et al., 1997; Dahms et al., 1998; Brown et al., 2002; Korossis et al., 2009; Martins et al., 2011; Zanetti et al., 2012; Barnes et al., 2015; Natali et al., 2015; Menzel et al., 2017; Seydewitz et al., 2017; Borsdorf et al., 2019; Philyppov et al., 2020) or biaxial tensile experiments (Baskin et al., 1994; Gloeckner et al., 2002; Nagatomi et al., 2004; Lu et al., 2005; Gilbert et al., 2008; Nagatomi et al., 2008; Toosi et al., 2008; Wang et al., 2009; Cheng et al., 2018; Morales-Orcajo et al., 2018; Trostorf et al., 2021). It should also be noted, that active tissue experiments are performed exclusively in the axial deformation state (Uvelius, 1976; Griffiths et al., 1979; Uvelius, 1979; Creed et al., 1983; Bramich and Brading, 1996; Menzel et al., 2017; Seydewitz et al., 2017; Borsdorf et al., 2019) to determine muscle-specific properties such as force–length and force–velocity relationships. The advantage of such experiments at tissue level is that the mechanical properties can be determined position- and layer-specific. However, these experiments are only suitable to a limited extent for investigating the mechanical functions of UBs in vivo, as the tissue is damaged during preparation. Therefore, observations on whole UBs during filling and micturition cycles are essential. Such a urodynamic examination technique, called cystometry, is preferred in clinical practice and there are active and passive examinations. Experimental studies in this field range from analyses using classical cystometry, in which a pressure sensor is inserted into the UB through the urethra and UB pressure is recorded during filling, to more advanced methods combining imaging techniques (Nenadic et al., 2013; Takezawa et al., 2014; Bayat et al., 2017; Gray et al., 2019). While ex vivo active experiments (Kaplan et al., 1991; Longhurst et al., 1991; Koo et al., 1995; Matsumoto et al., 2002; Lentle et al., 2015; Heppner et al., 2016) investigate the influence of stimulation, the role of the central nervous system and neurotransmitters, and detrusor contractility, in vivo passive experiments (Andersson et al., 1989; Wall et al., 1994; Rohrmann et al., 1997; Damaser, 1999; Lee and Yoon, 2013; Nenadic et al., 2013; Takezawa et al., 2014; Bayat et al., 2017; Kim and Hill, 2017; Rocha, 2017) aim to correlate the mechanical properties of the UBW with urodynamic studies and analyse the influence of obstruction, filling rates and organ transplant feasibility.

In the present study, we investigate the deformation of the whole UB during the active and passive experiments using five camera systems. In addition to the three-dimensional surface, pressure and UB volume are recorded either during filling or stimulated emptying against a defined back pressure. Active stresses in the UBW are estimated by assuming a spherical shape for the bladder in the activated state. The approach in the present study focuses exclusively on the bladder during the micturition phase without the influence of the urethra as in cystometry. The specific focus on the organ allows an isolated description of the contractile behaviour on the scale of the whole organ.

2. Materials and methods

2.1. Ethical approval

Experiments were carried out in accordance with the recommendations of the German animal welfare law (Tierschutzgesetz, BGBl. I 1972, 1277, section 8). The protocol of this study was approved by the competent authority for animal welfare in Thuringia, Germany (Landesamt für Verbraucherschutz (Abteilung Gesundheitlicher und technischer Verbraucherschutz); Permit Number: 02-001/15).

2.2. Urinary bladder preparation and experimental setup

For experimental investigations, six ($n = 6$) UB were removed from female domestic pigs (*Sus scrofa domesticus*) directly after their slaughter, and immediately transferred to the laboratory. For the measuring of the three-dimensional surface during the experiments, the ligaments and ureters were removed close to the UBW, see Fig. 1(a) and (b). All UBs were divided into 2 groups ($G_{1/2}$), see Table 1, which differed in how the three-dimensional surfaces were measured during the experiments. After measuring a passive filling cycle, the UBs of group G_2 were subjected to further tests (isovolumetric, isobaric) without any preconditioning. The UB from this group serve as a reference. In group G_1, the UBs were coated with an irregular pattern of black and white varnish dots prior to the active tests, see Fig. 1(c), and then dried. The pattern enables the reconstruction of the three-dimensional UB surfaces in a post-processing step.

The mechanical experiments were carried out in a 10-cornered basin with a diameter of about 800 mm, see Fig. 2. A syringe pump with a capacity of 50 ml was used to fill the UB. A height-adjustable scale measures the liquid expelled from the UB and sets a constant back pressure during the isobaric experiments, while a check valve prevents liquid from flowing back into the UB. To track the deforming UB surface during the testings, 5 camera systems, each consisting of 2 CMOS cameras (equipped with 45 mm lenses), were positioned at a distance of 840 mm around the UB. Polarised light with object filters was used to achieve the best possible illumination. The images were taken at a rate of 5 Hz. Using the digital image correlation method, a muscle surface reconstruction method used by the authors (Böl et al., 2013, 2015), the deforming bladder surface was evaluated after the measurements.

Activation of the smooth muscle tissue was done by direct activation with platinum electrodes. To create a homogeneous electric field, one electrode was placed in the centre of the UB and three electrodes were placed outside along the UBW. The stimulation was done with a constant voltage, which was determined in the isovolumetric setup at the reference volume, see Section 2.3.1. The voltage was stepwise increased (doubled) until the pressure did not increase by more than 3%. The determined voltage, multiplied by a factor of 2, was also sufficient for smaller filling quantities. The determined stimulation voltage varied within the UBs between 20 V and 40 V, see Table 1. The overall electrical resistance at the reference volume was 10 to 14 Ohm, increasing slightly at small filling volumes and up to 60% in fully contracted UBs. Stimulation was applied with a device capable of maintaining currents of up to 6 A. Pulses of width 0.5 ms were applied in alternating polarity with a frequency of 100 Hz, resulting in a duty factor of 0.5 (van Mastrigt and Glerum, 1985). A buffered solution (van Mastrigt and Glerum, 1985: 143 mM sodium, 1.9 mM calcium, 5.9 mM potassium, 1.18 mM magnesium, 126.5 mM chloride, 1.18 mM sulphate, 1.2 mM dihydrogen phosphate, 25.01 mM hydrogen carbonate, 11 mM glucose) provides an adequate environment and is flushed with 95% oxygen and 5% carbon dioxide, resulting in a pH of 7.4–7.45. The temperature was kept constant at 37 °C. A resting period of 5 min was maintained before each activation. During this time, the UB filling was kept at the reference volume to allow sufficient oxygenation and metabolite diffusion, as the UBW is thin at this volume.

2.3. Experimental investigations

2.3.1. Passive experiments

In a first step, before realising isovolumetric and isobaric experiments, passive experiments are carried out in which the UB is filled at a constant rate of 10 ml/min. The pressure is recorded at a rate of 10 Hz. Due to the capacity of the syringe, several cycles are required to reach a filled state of the UB. After the passive experiments, a reference volume (Table 1) was defined as the point at which the pressure–volume relation features a sharp increase after the plateau, see e.g. Fig. 3. This reference volume is used as the maximum capacity in further experiments.

Table 1
UBs used within this study.

Group	UB number	Reference volume [ml]	Voltage [V]	Geometry measurement
G_1	I	275	20	3D surface
	II	275	20	
	III	200	40	
	IV	250	30	
G_2	V	350	40	Silhouettes
	VI	160	30	

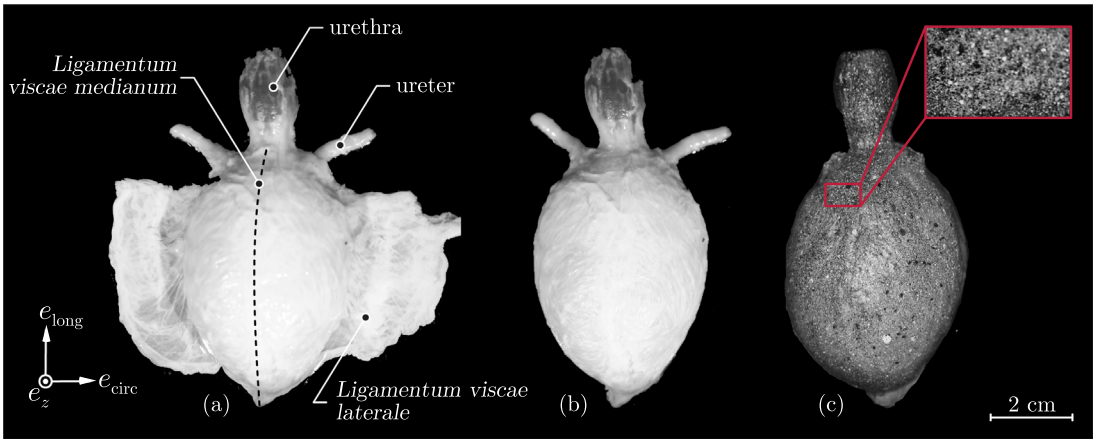

Fig. 1. UB during experimental processing: UB (a) dissected from the pig, (b) with removed ligaments, and (c) coated with black and white varnish.

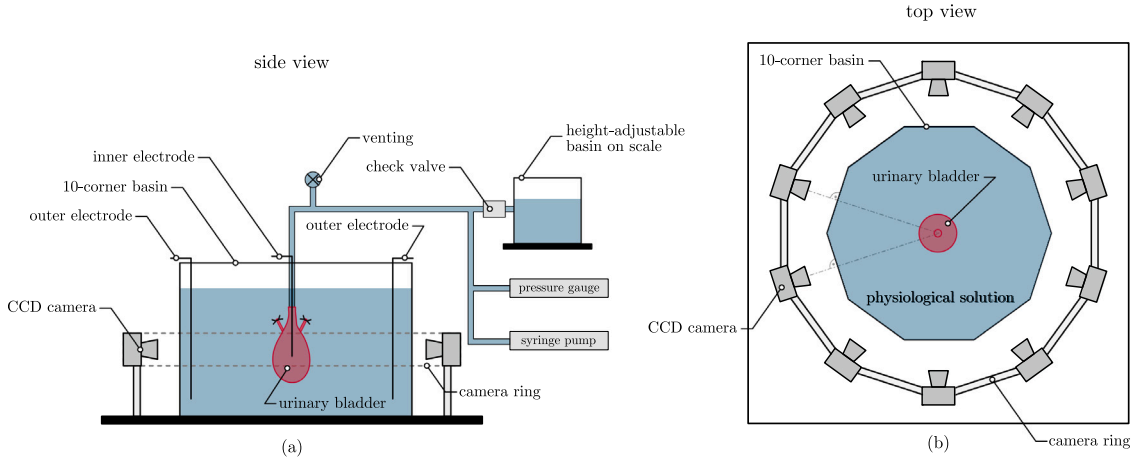

Fig. 2. Schematic illustration of the experimental setup: (a) Side view and (b) top view.

2.3.2. Active isovolumetric experiments

In isovolumetric experiments, UBs are first filled to reference volume, all connected valves are closed and a zero point measurement of the pressure is taken as a reference. In the next step, the pressure sensor is connected to the UB and records the pressure created by the passive filling. This is followed by a stimulation period of 15 to 25 s, followed by a relaxation period of 40 s. Data is collected at a rate of 1000 Hz. Starting from the reference volume defined in the passive test, the filling volume is gradually reduced to smaller volumes between different isovolumetric tests. As shown by Kaplan et al. (1991), the gradual decrease has no influence on the measurements. UBs with a high absolute reference volume can be tested at lower capacities, resulting in different experimental conditions.

2.3.3. Active isobaric experiments

In isobaric tests, a constant back pressure and an initial volume are specified. Each experiment starts with a zero point measurement of the pressure, followed by a measurement of the passive, unstimulated UB at filled volume, as is done in isovolumetric tests. Then the UB is stimulated and the pressure and outflow are measured at a rate of 1000 Hz. The stimulation time is adjusted until there is no more outflow, resulting in activation of up to 85 s. The tests are carried out at filling conditions of 100%, 75%, 50%, and 25%. The back pressures vary between 37.5 and 1.5 cmH_2O.

2.4. Data analysis

Since the measurement data contain different numbers of measurement points and discontinuities due to the changing of the infusion syringes, the data were processed in a post-precessing step. Passive pressure curves were averaged over a 5 s interval by calculating the median (*movmedian* function, MATLAB R2019b, The MathWorks, Inc.) and interpolated at grid points between refill cycles, while active measurements are averaged along an interval of 0.5 s, corresponding to 50 data points.

Based on the active isovolumetric experiments, the active force

$$F_{act} = p_i \pi r^2 \quad \text{with} \quad r = \left(\frac{3}{4\pi} V_{fill}\right)^{1/3} \tag{1}$$

is calculated as a function of the maximum pressure p_i inside the UB, the applied liquid volume V_{fill} (Uvelius and Gabella, 1980). Based on the spherical shape of the filled UB, this evaluation approximates the UB as a sphere and the density of the UBW is assumed to be incompressible due to the high cellular fluid content (Natali et al., 2015). In the present study, the UBW thickness is approximated by a homogeneous layer around the filling volume with a volume equal to the volume of the UBW ($V_{UBW} = m_0/\rho_{UBW}$) and a density of $\rho_{UBW} = 1.05$ (Speich et al., 2007; Murphy, 2011; Murtada et al., 2012). The calculated radius reflects the inner surface of the UB.

The active stress

$$\sigma_{act} = \frac{F_{act}}{A} \quad \text{with} \quad A = \pi(2rt + t^2) \tag{2}$$

is calculated by dividing the active force F_{act} by the area A of the bladder tissue, whereby

$$t = \left(\frac{3(V_{fill} + V_{UBW})}{4\pi}\right)^{1/3} - r \tag{3}$$

defines the thickness of the UBW. According to the described method, thicknesses for the 0% fill state are extrapolated between 4.6 and 7.2 mm, corresponding to the range of regionally dependent wall thicknesses between 3.1 and 7.5 mm (Seydewitz et al., 2017; Morales-Orcajo et al., 2018).

As geometric descriptors, the stretches

$$\Lambda_{circ} = \frac{r^{act}_{circ}}{r^{pas}_{circ}} \quad \text{and} \quad \Lambda_{long} = \frac{r^{act}_{long}}{r^{pas}_{long}} \tag{4}$$

in circumferential and longitudinal directions are introduced, enabling a description of the active contraction. Note, the indices 'act' and 'pas' describe the active and passive state of the UB, respectively. Λ_i therefore represent mean stretches measured along the two axis of the UB. To describe the shape in the active or passive state, the diameter ratios

$$\Gamma^{pas} = \frac{r^{pas}_{long}}{r^{pas}_{circ}} \quad \text{and} \quad \Gamma^{act} = \frac{r^{act}_{long}}{r^{act}_{circ}} \tag{5}$$

in the two axes of the ellipse are formulated. Their difference $\Delta\Gamma$ represents the change in shape independent of the volume; a value of 0 represents a constant shape, while positive values indicate a disproportionately high contraction in the longitudinal direction.

3. Results

3.1. Pressure–volume relationship

The results of the passive filling processes are shown in Fig. 3(a) in the form of pressure–volume relations. Basically, a strong pressure increase can be seen up to a volume of about 25 ml, until a plateau is reached at 2.5 to 4 cmH_2O. At higher volumes, the pressure increases sharply with volume. While the plateau pressure is similar, the sharp increase starts between 160 and 350 ml for different bladders. The reference condition of a filled UB, defined here as the point of sharp pressure increase after plateau, is shown in Table 1, and defined as 100% relative volume. Finally, Fig. 3(b) shows the mean and standard deviation as a function of relative volume. Large peaks in the standard deviation only occur due to the refilling process of the syringe. The general shape of the curve is constant for all measurements, resulting in small deviations.

3.2. Active experiments

Active experiments were performed at different voltages ranging from 20 to 40 V, see Table 1. These values are smaller than in experiments UB of rabbits (Kaplan et al., 1991; Matsumoto et al., 2002) or foetal calves (Koo et al., 1995), where voltages of 80 V were used. However, we attribute this difference to the large surface of our stimulation electrodes, leading to a low overall resistance at the electrode surface.

3.2.1. Isovolumetric experiments

Fig. 4(a) shows the internal bladder pressure during activation for different filling volumes relative to the reference volume. Thereby, the pressure in the UB decreases with increasing filling level. Comparing the two groups considered in this study, a clear difference can be seen. Thus, the UBs of group G_1 have a pressure of 22.3 cmH_2O at a relative volume of 15%, while the pressure of group G_2 is 72.7 cmH_2O at an identical relative volume. Based on these pressures, the active stress–volume relationships are shown in Fig. 4(b). There are also clear differences between the two groups. Thus, the UBs of group G_1 and G_2 feature an average stress of 34.48 kPa and 64.96 kPa, respectively, at 100% relative filling. In addition, in UBs III and IV, the varnishing procedure was shown to reduce the pressure by ~42% in isovolumetric contractions at 100% reference volume in both cases. However, although there are clear quantitative differences between the two groups in both the pressure-filling and stress-filling volume relationships, the curves of the two groups are each qualitatively similar.

3.2.2. Isobaric experiments

In isobaric experiments, the back pressure is constant while the fluid volume is pushed out of the UB due to a higher pressure. The results of a single experiment, cf. UB VI in (Table 1) are shown in Fig. 5(a–c). The experiment starts with a relative volume of 100% and the back pressure varies between 5 and 37.5 cmH_2O. The internal bladder pressure is shown in black, while the constant back pressure is indicated by a dashed green line. As long as the internal bladder pressure is higher than the back pressure, outflow can be observed, indicated by a positive slope of the cumulative outflow, shown in red. Some experiments show a decrease in emptied fluid after longer stimulation times. Note, the stimulation time is shown as a light grey area.

The data from all experiments are summarised in Fig. 5(d), where the maximum ejected volume is plotted as a relative value to the reference over the relative starting volume. The dashed black line marks the theoretical value of a completely emptied bladder. At small back pressures (1.5–5 cmH_2O), indicated by the number next to the curve, the theoretically possible volume is emptied. Higher pressures reduce the emptied volume, especially for relatively large volumes. As indicated in isovolumetric experiments, a smaller filling state leads to higher active pressures within the bladder, which allow emptying despite high back pressures.

The maximum pressures exerted in the isobaric test do not reach the values possible in the isovolumetric test, except at large relative volumes and back pressures. At low back pressures, the values remain with a larger margin above the back pressure, which accelerates the outflow. Fig. 6 shows the pressure difference between the maximum pressures measured in the isobaric test (marked in red) and the corresponding isovolumetric pressures (empty circles). While the UBs of group G_1 are close to the isovolumetric pressure in the isobaric tests, those of group G_2 show a high pressure difference. Different colours represent tested UB.

To assess the actual driving force of outflow from the UB, Fig. 6 focuses on the pressure difference between the maximum active pressure achieved in isovolumetric and isobaric experiments for two different filling conditions. Matching pressure states are represented by vertical black lines. As shown in Fig. 6(b), the pressure difference tends to

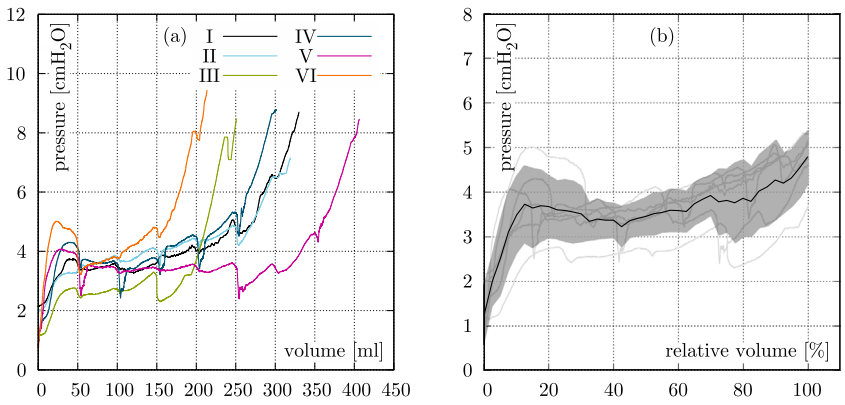

Fig. 3. (a) Pressure–volume relationship for each experiment and (b) mean pressure (black curve) and standard deviation (shaded grey area) for the relative volume. Note, the light grey curves indicate the data of the single experiments.

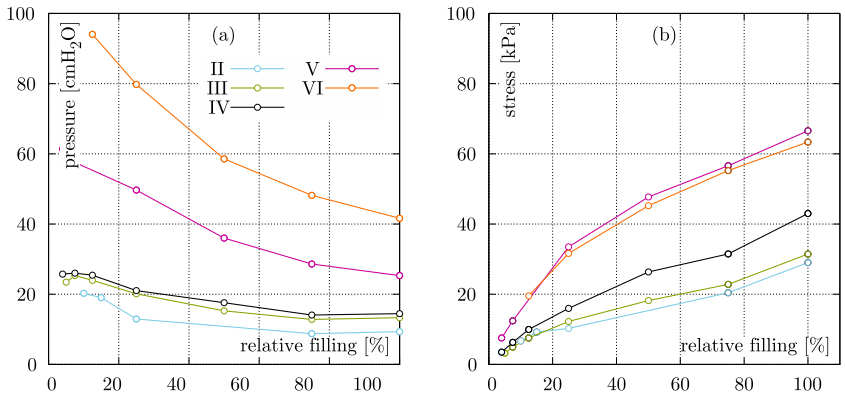

Fig. 4. Isovolumetric experiments: (a) Active pressure and (b) stresses as function of the relative filling of the UBs. Note, to guide the eyes, the points are connected with solid lines.

decrease at higher back pressures. Interestingly, the pressure difference between the maximal isobaric pressure and the back pressure is almost constant for both filling levels, see Fig. 6, while the difference to the theoretically possible pressure from isovolumetric experiments increases with lower filling volumes.

3.3. Urinary bladder surface deformation measurements

In addition to the determination of pressure–volume and stress–volume relationships, a key point of this study is the determination of the UB surface during active and passive deformations.

As a typical example, Fig. 7 shows a reconstructed UB (UB II, Table 1) at different, discrete time points during the isovolumetric experiment for a reference volume of 100%. The surfaces were reconstructed at the beginning (t_1), at maximum internal pressure during activation (t_2), at the end of stimulation (t_3) and after a relaxation time of about 40 s (t_4). The images show a change in shape from an ellipsoid at the beginning to a spherical shape at maximum pressure. This is confirmed for all measurements (G_1 and G_2) as the mean ratio of longitudinal to circumferential diameter decreases from 1.24 ± 0.12 to 1.06 ± 0.08 for the 13 isovolumetric experiments, as shown in Fig. 8. While there is no dependency observed in the passive state for the ratio of radii, in the active state a trend towards a larger radius in longitudinal direction can be seen. In the passive state, an almost constant ellipsoidal shape is maintained across different filling states. In the active state, on the other hand, the spherical shape is more likely to be achieved for smaller relative volumes, which are also the category of higher pressures and make it more likely to achieve the shape with a minimum surface area. Later during activation, the pressure decreases and the shape becomes ellipsoidal. Even after a short relaxation time, the shape does not return to its initial state. During isovolumetric experiments, the optically measured bladder volumes remain almost constant, i.e., 292.74, 291.91, 293.34, and 292.58 ml for measurement points (t_1), (t_2), (t_3), and (t_4), respectively, thus validating the measurement procedure implemented here.

In isobaric experiments, the UB contracts spherically, but the final state is elliptical, regardless of the residual fluid. The initial and final state of an isobaric experiment with an initial relative capacity of 100% and a low back pressure of 1.5 cmH_2O are shown in Fig. 9. The residual liquid is about 5% of the initial volume, as shown in Fig. 5(b).

To assess the influence of the varnish, Fig. 10 shows various geometric changes depending on the groups G_1 and G_2. Fig. 10(a) shows the elongation in longitudinal over circumferential direction. These strains were measured as the ratio of the diameters of the entire bladder in the active and passive states in isovolumetric experiments. After performing a Kolmogorov–Smirnov test and a subsequent t-test, no significant ($\alpha = 0.5$) difference can be detected between the two groups. The change in the ratio between active and passive state describes the ability to contract and is shown in Fig. 10(b). The change is mainly dependent on the ratio before contraction, but statistically significant differences between samples with and without varnish are not visible (Mann–Whitney U-test, $\alpha = 0.5$).

4. Discussion

The reference volume, defined in the present study at the point of pressure rise after the plateau in the volume-pressure curve (Koo et al., 1995), is relatively low compared to other studies. Kaplan et al. (1991) used double the pressure of the plateau to assess the reference volume. In the present study, this would have resulted in approximately 30%

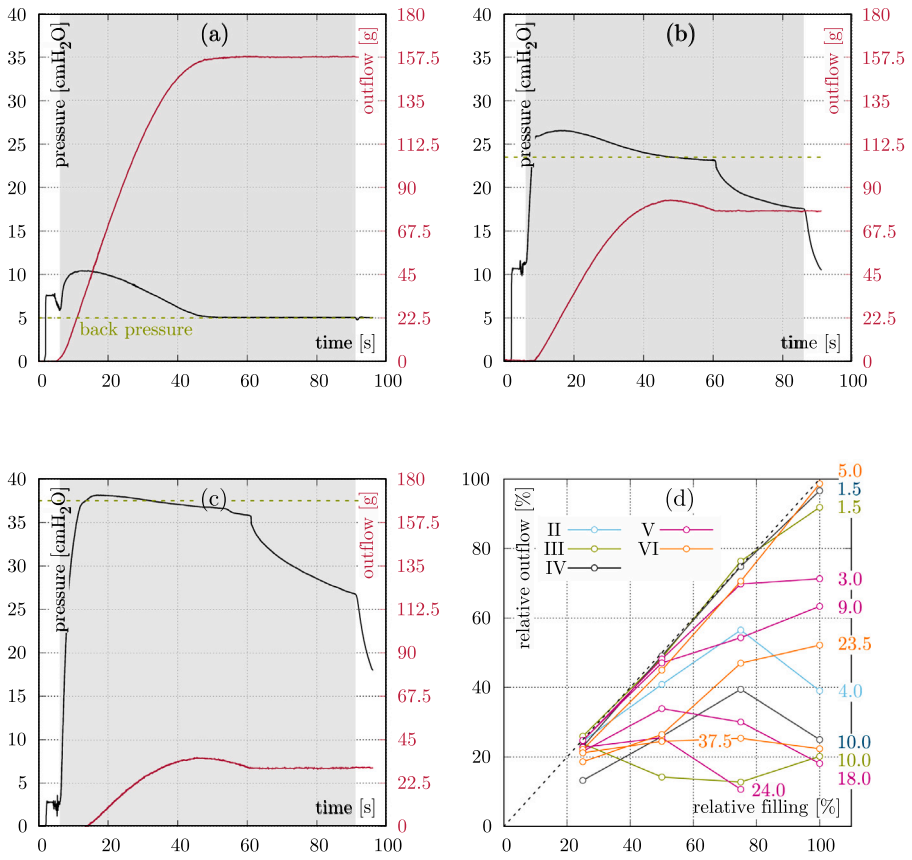

Fig. 5. Results of the isobaric experiments: Individual isobaric experiments (UB VI, cf. Table 1) for back pressures (see green dashed lines) of (a) 5 cmH_2O, (b) 23.5 cmH_2O, and (c) 37.5 cmH_2O. Note, the grey shaded areas indicate the period of UB activation. (d) Outflow relative to the reference filling as a function of the relative filling for all experiments. The pressure (unit: cmH_2O) is indicated by the number next to the respective curve. The dashed black line indicates the maximum theoretical outflow.

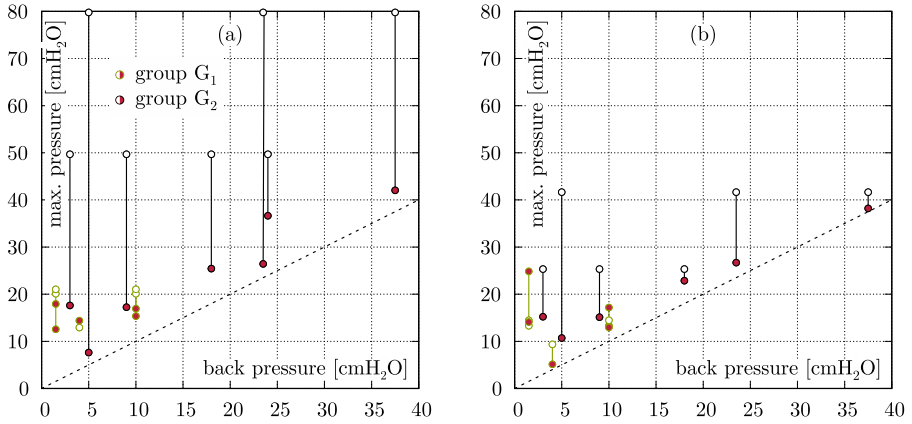

Fig. 6. Maximum pressure of isobaric (red filled cycles) and corresponding isovolumetric (empty circle) experiments for different relative fills and back pressures for UB filling levels of (a) $V = 25\%$ and (b) $V = 100\%$. The dotted line indicates the point of equal pressures. Black vertical lines indicate the pressure difference between isobaric and isovolumetric experiments.

higher volumes. This difference is not critical as the relative volumes are only compared within this study.

In general, it can be observed that the varnish leads to a change in the measured values of the differential pressure, see Fig. 4. It remains unclear whether this effect is caused by the varnish itself or by the accompanying drying step, which was necessary to fix the varnish on the bladder surface. No difference in bladder deformation can be seen in the measurements, cf. Fig. 10. Due to the small number of bladders in each group, no statistical aid can be used. Nevertheless, the recorded strains in the active state seem to agree for measurements with and without varnish. The same behaviour is observed for the difference in the ratio of longitudinal to circumferential diameter between the active and passive states. Therefore, the optical data collected for bladder deformation analysis does not seem to be affected by the varnish. In summary, it is therefore advisable to separate the mechanical and optical measurements.

4.1. Passive experiments

Passive tests were performed without varnish and are evaluated without regard to differences in this parameter. The typical response of

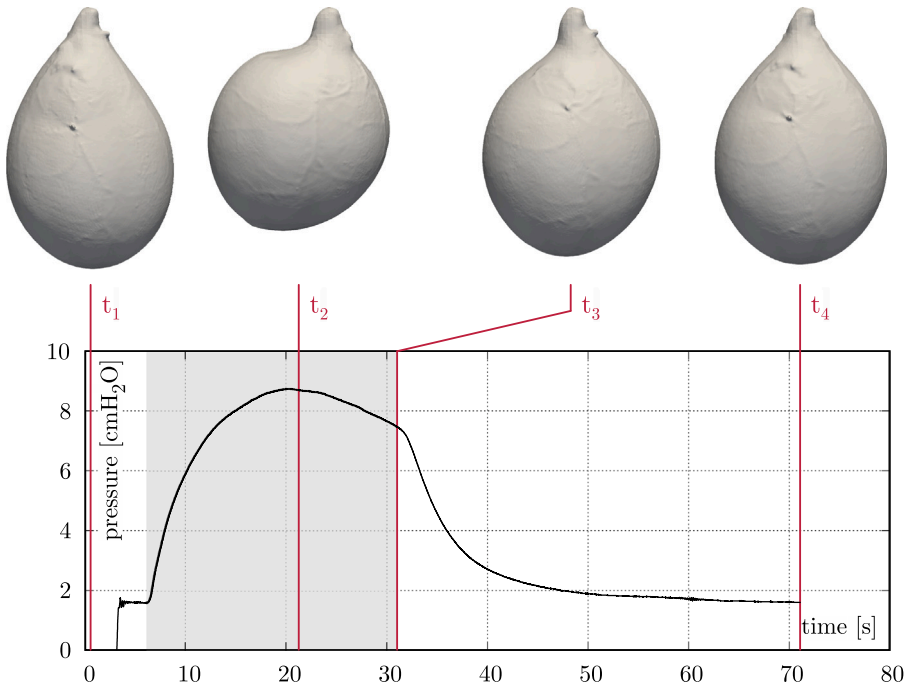

Fig. 7. Exemplary isovolumetric experiment (UB II, Table 1) at a capacity of 100%. Three-dimensional surfaces of the UBs are reconstructed at four discrete points $t_{1/2/3/4}$ = 0.2/20.1/31.1/71.2 s. Note, the grey shaded area indicates the period of UB activation.

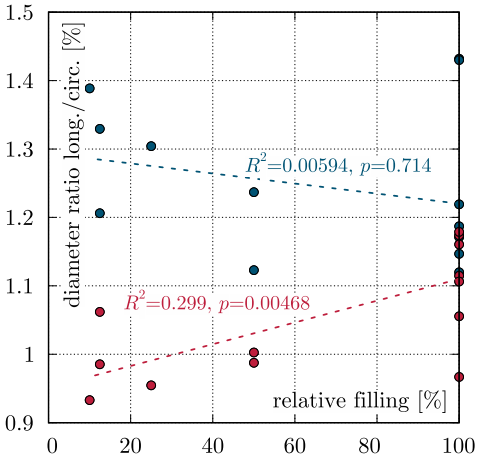

Fig. 8. Ratio of diameter in longitudinal to circumferential direction for the passive state (blue) and at the maximum pressure during activation (red) of the UB during isovolumetric experiments. The dashed lines represent linear regression lines (given are the determination coefficient R^2 and the significance level p).

a pressure plateau (Fig. 3) as commonly observed in the UB was measured (Parekh et al., 2010). The constant pressure of 2.5 to 4 cmH_2O is within the range of measurements in rats (2 cmH_2O) and sedated pigs (14 cmH_2O (Mills et al., 2000a)). The filling rate of Mills et al. (2000a) is 5 times higher than that used in the present study, which may explain the deviation to higher pressures. The measured plateau pressures are independent of the bladder size, leading to the conclusion that this pressure could be the ideal working range for the UB of pigs.

Compliance measured to the end of plateau in the present study ranged from 30 to 87.5 ml/cmH_2O, which is comparable to values measured in pigs (Mills et al., 2000b) and humans (Toppercer and Tetreault, 1979) and validates their use for the following active test.

4.2. Isovolumetric experiments

During the isovolumetric experiments, an increase in pressure is found for decreasing filling volumes, see Fig. 4. The same behaviour was observed in rabbits (Kaplan et al., 1991) and guinea pigs (Uvelius and Gabella, 1980). The active pressure of G_2 (72.7 cmH_2O) is above that of G_1 (22.3 cmH_2O), but close to measurements of Parsons et al. (2012) (63.2 ± 3.6 cmH_2O), who maintained physiological conditions throughout the experiment. Similar maximal pressures therefore indicate a sufficient supply of nutrients for G_2. Within the present study, the assumption of a spherical UB shape of the bladder was used to evaluate the peak stresses in the UBW and is valid due to the diameter ratio of 1.06 ± 0.08, which was accessed when measuring the deformation. The change to a spherical shape offers the advantage of a more homogeneous load absorption over the UBW and a lower circumferential stress due to a reduction of the longitudinal length. This spherical shape is also observed in human bladders during urodynamics (Gray et al., 2019).

With regard to the stresses, an opposite behaviour can be seen, i.e., the stress increases with increasing volume. This can be explained by the reduction of the thickness of the UBW, as the thickness is a function of $V^{1/3}$, and the Cauchy stress is evaluated accordingly.

Due to different deformations, the isovolumetric experiments cannot be directly compared with uniaxial isometric experiments. In Uvelius (1976), no maximum stresses were measured up to a stretch of 3, while Seydewitz et al. (2017) found maximum stress values at an optimum stretch of 2.8. Furthermore, an optimal filling volume (for maximum pressure generation) was found by Uvelius and Gabella (1980), whereby this only occurs for very low filling states (UB II to IV, Fig. 4(a)). A maximum active stress is not found due to the definition of the reference volume, as the present study stops before the steep passive pressure rise after the plateau, see Fig. 3(b). The subtraction of the passive stresses does not contribute to any significant extent until after this point and a decrease in Fig. 4(b) is therefore not measured. However, the observed range of volumes is already high, while the observed strains are comparatively low due to their relation

$$\lambda \propto \frac{r}{r_0} \propto \left(\frac{V}{V_0}\right)^{1/3}. \tag{6}$$

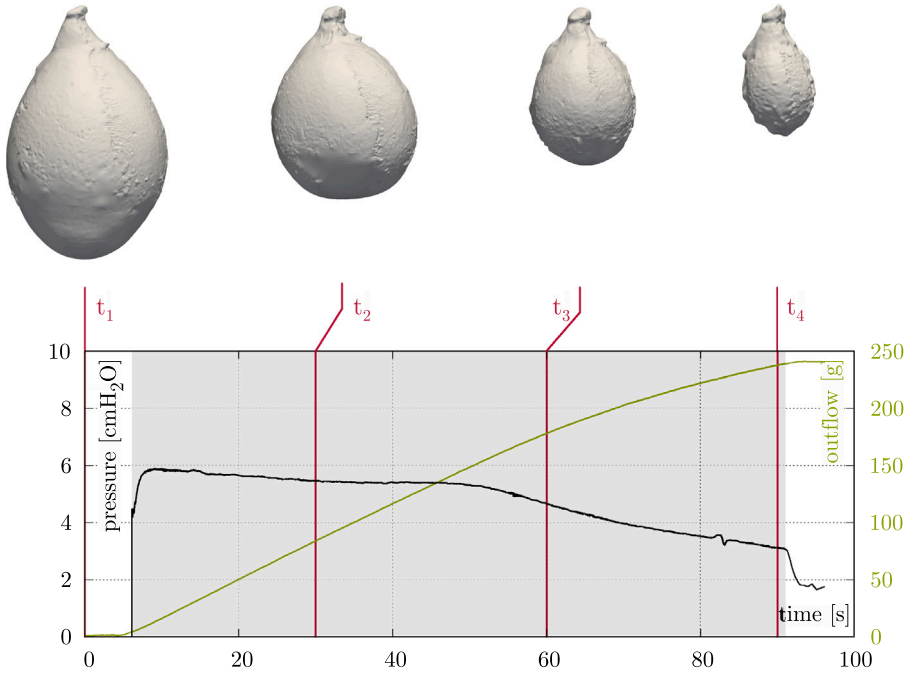

Fig. 9. Exemplary isobaric experiment (UB IV, Table 1) at a capacity of 100% and a back pressure of 1.5 cmH_2O. Three-dimensional surfaces of the UBs are reconstructed at four discrete points $t_{1/2/3/4}$ = 0/30/60/90 s. Note, the grey shaded area indicates the period of UB activation. Further, the black line represents the active pressure over time, while the expelled liquid is displayed in green.

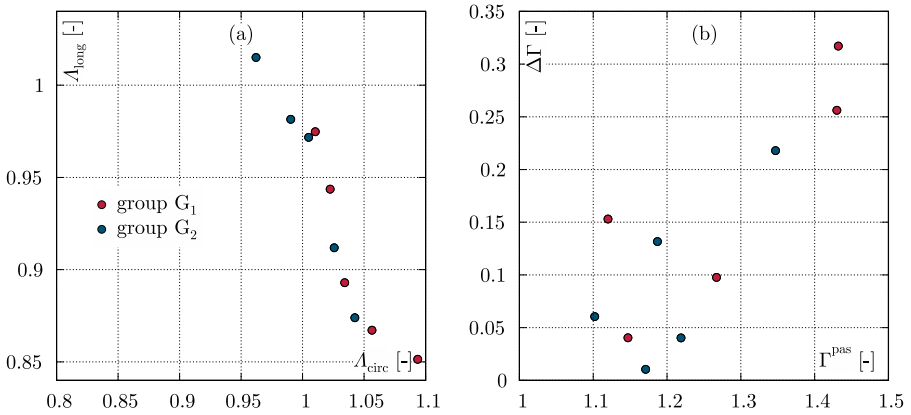

Fig. 10. Influence of the varnish on the mechanical behaviour: (a) Stretches in longitudinal over circumferential directions for a relative filling volume of 100%. G_1 and G_2 represent the groups defined in Table 1. (b) absolute change in ratio between longitudinal and circumferential direction displayed over the same ratio prior to the experiment.

Finally, the approximately equal active tensions in the measurements of the UBs without varnish of 65 kPa, despite their large difference in reference volume (160 and 350 ml), suggest a possible use as a reference value for comparing the active properties of normal and abnormal UBs.

4.3. Isobaric experiments

In the case of isobaric experiments, the characteristics of pressure over time during a contraction are similar to those measured in cystometry under physiological conditions with an induced partial obstruction (Mills et al., 2000b). Deviations are due to the different method of implementing a higher back pressure. The method chosen in the present study can only lead to a minimum pressure inside the bladder similar to the applied back pressure, whereas in an obstructed urethra, due to pathological conditions (e.g., partial bladder obstruction), the back pressure is defined by the flow resistance. Compared to obstructions, bladders can be deflated to a greater extent at low flow rates due to the low back pressures. In future experiments, obstruction can be mimicked by a choke with changing diameter. Nevertheless, the data presented allow a comparison to the isovolumetric experiments.

The high pressures achieved in isovolumetric experiments are not observed in the isobaric experiments, as seen in Fig. 6, except at high volumes and back pressures. Reduced isobaric pressures can be explained by the force–velocity relation of UB smooth muscle tissue (Menzel et al., 2017), as UB emptying is driven by muscle shortening. Furthermore, force during muscle shortening might be reduced by contraction history effects (Abbott and Aubert, 1952; Siebert et al., 2015). E.g., residual force depression (rFD), i.e., the reduction of isometric muscle force after muscle shortening compared to an isometric reference contraction at the same muscle length, has been reported for different smooth muscle tissues (Gunst, 1986; Tomalka et al., 2017) including UB tissue (van Asselt et al., 2007; Menzel et al., 2017). During the isobaric experiment, see Fig. 9, the smooth muscle tissue shortens continuously while the urine outflow increased until the end of stimulation. Due to shortening induced rFD reported for UB tissue

strips (Menzel et al., 2017) and UB muscle fibre bundles (van Asselt et al., 2007) we expect likewise history effects for entire UB contractions. However, quantification of rFD for the entire UB would require a combination of an isobaric contraction followed by an isovolumetric contraction, while the UB is continuously stimulated. An equivalent to rFD could then be calculated as the pressure difference between the isovolumetric phase after the isobaric contraction and an additional isovolumetric reference contraction against the same UB volume. As we performed only isobaric and isovolumetric experiments in this study, we cannot give an exact statement on the relevance of history effects on entire UB organ level. This has to be addressed in future studies.

It can be assumed that the outflow is not limited by the pressure but rather by the contraction speed of the smooth muscle cells. The pressures within the bladder only reach states slightly higher than the back pressure. This is underlined by the time required to reach maximal pressures in isovolumetric tests after stimulation (18.5 ± 6.2 s), which can also be seen in Fig. 7. The flow rates in isobaric experiments do not show a clear trend except for their dependence on the pressure gradient, which can be seen in Fig. 6 as the difference between red markings and the dashed black line.

4.4. Functional aspects on relation to mechanical finding

The UB exhibits an ellipsoidal shape in the passive unfilled state. This ellipsoidal shape is maintained during the passive filling, see Fig. 1(b) and Fig. 7 at t_1. The passive resistance of the bladder during filling is relatively low over a wide range, see Fig. 3(b). Maintaining a low pressure for a wide range of volumes offers different advantages. First, the stress on the material is very low, resulting in a low risk of damage. Secondly, the pressure in the UB represents the back pressure of the kidney and obstruction of urine flow to the UB can cause hydronephrosis (Gakhar et al., 2009).

Nevertheless, during activation, the bladder shape changes from ellipsoidal to spherical, see Fig. 7 at t_2. This might be induced by slightly higher active forces generated by the UBW in the longitudinal compared to the circumferential direction (Seydewitz et al., 2017; Borsdorf et al., 2019). These results can be explained by histological analysis, yielding a higher amount of muscle fibres in the longitudinal direction compared to the circumferential direction (Borsdorf et al., 2019). However, normalisation of active forces by the corresponding cross-sectional area did not reveal any differences in tension of the longitudinal and circumferential muscle layers. Furthermore, there were no differences in active muscle properties (force–length and force–velocity relation) between the longitudinal and circumferential muscle layer (Borsdorf et al., 2019). No differences in active properties will support a homogeneous deformation of the spherical bladder during contraction. Moreover, as mentioned in Section 4.2, the spherical shape of the UBs lead to a more homogeneous stress field during activation than an elliptical shape. This deformation is consistent with the preferred fibre orientation in the ventral part in longitudinal direction, especially in the stretched state (Trostorf et al., 2021).

In contrast to the stomach, which autonomously stores, digests, and transports its content (Bauer et al., 2020), the UB is either in the process of passive filling or active micturition. Thus, similar properties of the circumferential and longitudinal muscle layers and lower locational differences in the UBW structure (Morales-Orcajo et al., 2018; Borsdorf et al., 2019), compared to e.g. the stomach wall (Bauer et al., 2020), allow the bladder for perfectly fulfilling its function, i.e., uniform spherical deformation coupled with continuous pressure generation. Therefore, the bladder is a suitable example for the interplay of structure and biomechanical properties to enable organ function.

4.5. Impact on three-dimensional urinary bladder modelling

The data recorded in the present study lead to a better understanding of the load transfer mechanisms (Seydewitz et al., 2017; Borsdorf et al., 2021) in the UB and can be used in particular to validate material models developed, e.g., based on tissue strip experiments. The three-dimensional geometry and matching pressure–volume curves provide all the information needed for a finite element simulation. Models for active properties, e.g., Seydewitz et al. (2017), can be validated at organ level.

In order to demonstrate the basic procedure, isobaric data generated here were used for an initial adjustment of a three-dimensional active model (Seydewitz et al., 2017). For this purpose, we used the material parameters identified in Seydewitz et al. (2017) to re-simulate the isobaric experiment of UB IV, see Table 1. Detailed information on the simulation (meshing, fibre orientations, boundary conditions) are given in the supplementary material. Fig. 11 shows the first results in the form of comparisons between the experiments and the simulation. In (b) the comparison between experiment and simulation during the passive filling phase is shown. As can be seen, the model cannot accurately represent the pressure–volume curve. The reason for this seems to be the way the parameters were identified in Seydewitz et al. (2017). Axial tensile experiments were used for parameter identification in Seydewitz et al. (2017), whereas during the passive filling phase the UBW is primarily loaded biaxially. In general, stresses obtained in uniaxial experiments feature lower stress values compared to those in biaxial experiments. Thus, the identified material parameters seem to lead to lower pressures at the same volume in the simulations, see Fig. 11(b). The isobaric contraction is shown in Fig. 11(a) in terms of the UB geometry, with experiments shown in grey and simulations in green. While the passive state is overestimated in the circumferential direction in the simulation (left), this difference becomes smaller during activation but remains (right). Basically, however, a good agreement qualitative between the experimentally measured volumes and the simulated ones can be seen. When the stress in the UBW increases in the active phase of the isobaric experiment, a spherical shape (same radius in longitudinal and circumferential direction) becomes visible, see Fig. 11(c), which agrees with the experimental results.

In summary, the data collected in this pilot study represent promising data set useful for model validation, among other applications. In a first non-calibrated comparison, it could be shown that the model developed in Seydewitz et al. (2017) is able to reproduce qualitatively the passive and active phases of the isobaric cases. However, further research is required to match all the experimental measurements quantitatively, like extended material parameter identification test, biaxial instead of uniaxial, among other factors.

4.6. Limitations of the study

In the present study, the reference volume is defined at the end of the pressure plateau during passive filling. This leads to an evaluation limited to the ascending part of the stress–volume relationship. Higher volumes would have been possible, but preventing tissue damage was considered a higher priority. Further, the geometry measurements are limited to the outer surface. Therefore, the evaluation is limited by the assumption of a homogeneous thickness over the entire UBW, even if data on tissue sections indicate regional differences (Morales-Orcajo et al., 2018). The realisation of a constant back pressure allows a good interpretation of the results. In nature, obstructions and thus a flow-dependent back pressure cause an increased pressure in the bladder (Jorgensen et al., 1983; Rohrmann et al., 1997). Finally, the ex vivo experiments are limited as the UB was not in contact with other organs and the hydrodynamic contribution of the urethra was not considered, which are non-negligible factors (Yang et al., 2014).

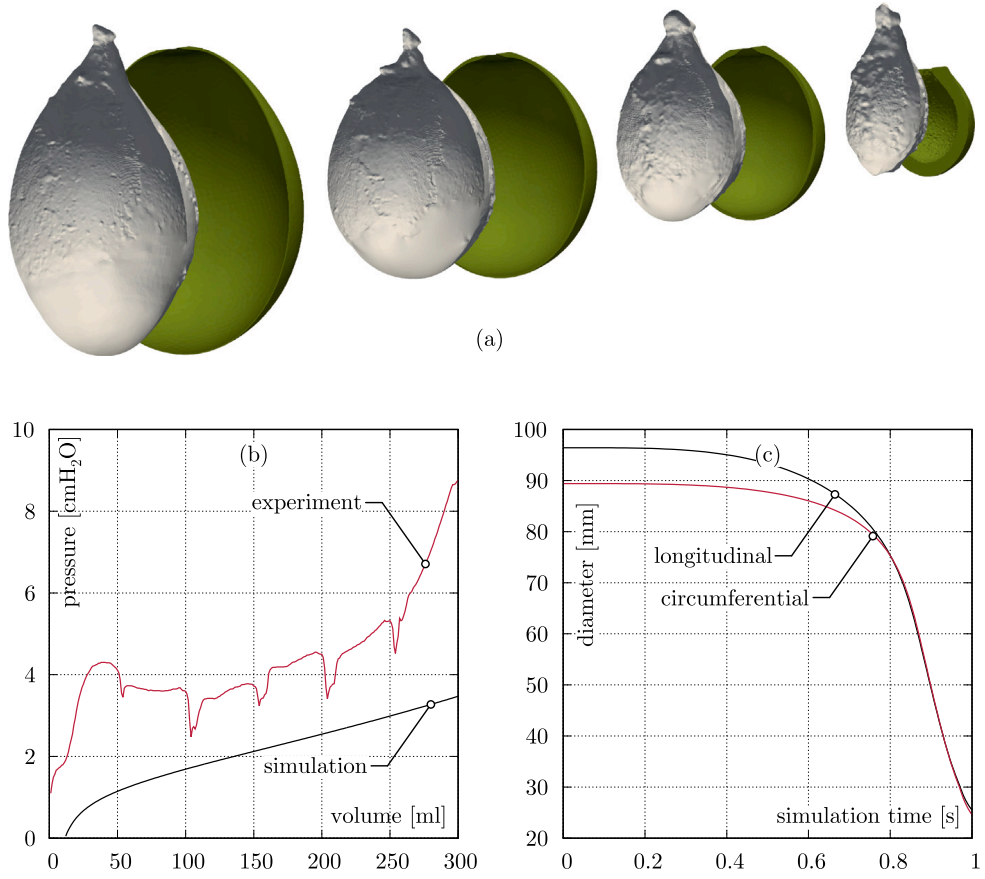

Fig. 11. First comparisons between experiment (present study) and simulation (based on the model developed in Seydewitz et al. (2017)): (a) Geometric changes during isobaric contraction (grey: experiment, green: simulation), (b) pressure–volume curve during the passive filling phase and (c) diameter of UB in longitudinal and circumferential direction during the isobaric contraction phase.

5. Conclusions

The data set collected in the present study supports research on passive and active properties of the UB. Measurements of the exact geometry with varnish influence the tissue and change its mechanical properties. Nevertheless, distinct mechanical properties are preserved. Stimulation of the bladder leads to longitudinal contraction from an elliptical to a spherical state, indicating a homogeneous stress field. Isovolumetric experiments show a strong dependence of the filling volume on the generated pressure. This explains the results of Jorgensen et al. (1983), in which smaller volumes were found for obstructed bladders, since this effect allows higher pressures. A rapid fatigue process is observed in isovolumetric experiments, which seems to be the dominant factor in isobaric experiments, since only partial emptying occurs. In addition, the outflow is limited by the contraction speed of the smooth muscle, as the pressure inside the UB is lower in isobaric experiments than in the previously measured isovolumetric tests.

CRediT authorship contribution statement

Robin Trostorf: Writing – review & editing, Writing – original draft, Validation, Methodology, Formal analysis. **Enrique Morales Orcajo:** Writing – review & editing, Methodology, Formal analysis, Data curation. **Amelie Pötzke:** Writing – review & editing, Investigation, Formal analysis, Data curation. **Tobias Siebert:** Writing – review & editing, Funding acquisition. **Markus Böl:** Writing – review & editing, Writing – original draft, Visualization, Validation, Supervision, Project administration, Methodology, Funding acquisition, Data curation, Conceptualization.

Declaration of competing interest

The authors declare that they have no known competing financial interests or personal relationships that could have appeared to influence the work reported in this paper.

Acknowledgements

Partial support for this research was provided by the Deutsche Forschungsgemeinschaft (DFG), Germany under Grants 244579774 and 386349077. The authors would like to thank Prof. R. Blickhan for the support within this research project, O. Till for the realisation of the experiments, and R. Bark for assisting in the construction of needed electrical parts for stimulating the tissue.

Appendix A. Supplementary data

Supplementary material related to this article can be found online at https://doi.org/10.1016/j.jmbbm.2022.105347. Supplementary material for the numerical simulations in form information of the meshing, fibre orientation, and boundary conditions can be found in the online version of the article.

References

Abbott, B.C., Aubert, X.M., 1952. The force exerted by active striated muscle during and after change of length. J. Physiol. 117 (1), 77.

Andersson, K.E., Arner, A., 2004. Urinary bladder contraction and relaxation: Physiology and pathophysiology. Physiol. Rev. 84 (3), 935–986.

Andersson, S., Kronström, A., Bjerle, P., 1989. Viscoelastic properties of the normal human bladder. Scand. J. Urol. Nephrol. 23 (2), 115–120.

Balthazar, A., Cullingsworth, Z.E., Nandanan, N., Anele, U., Swavely, N.R., Speich, J.E., Klausner, A.P., 2019. An external compress-release protocol induces dynamic elasticity in the porcine bladder: A novel technique for the treatment of overactive bladder? Neurourol. Urodyn. 38 (5), 1222–1228.

Barnes, S.C., Shepherd, D.E.T., Espino, D.M., Bryan, R.T., 2015. Frequency dependent viscoelastic properties of porcine bladder. J. Mech. Behav. Biomed. Mater. 42, 168–176.

Baskin, L., Meaney, D., Landsman, A., Zderic, S.A., Macarak, E., 1994. Bovine bladder compliance increases with normal fetal development. J. Urol. 152 (2), 692–695.

Bauer, M., Morales-Orcajo, E., Klemm, L., Seydewitz, R., Fiebach, V., Siebert, T., Böl, M., 2020. Biomechanical and microstructural characterisation of the porcine stomach wall: Location- and layer-dependent investigations. Acta Biomater. 102, 83–99.

Bayat, M., Kumar, V., Denis, M., Webb, J., Gregory, A., Mehrmohammadi, M., Cheong, M., Husmann, D., Mynderse, L., Alizad, A., Fatemi, M., 2017. Correlation of ultrasound bladder vibrometry assessment of bladder compliance with urodynamic study results. PLoS One 12 (6), e0179598.

Blanker, M.H., Groeneveld, F.P.M.J., Bohnen, A.M., Bernsen, R.M.D., Prins, A., Thomas, S., Ruud Bosch, J.L.H., 2001. Voided volumes: normal values and relation to lower urinary tract symptoms in elderly men, a community-based study. Urology 57 (6), 1093–1098.

Böl, M., Leichsenring, K., Ernst, M., Wick, C., Blickhan, R., Siebert, T., 2015. Novel microstructural findings in m. plantaris and their impact during active and passive loading at the macro level. J. Mech. Behav. Biomed. Mater. 51, 25–39.

Böl, M., Leichsenring, K., Weichert, C., Sturmat, M., Schenk, P., Blickhan, R., Siebert, T., 2013. Three-dimensional surface geometries of the rabbit soleus muscle during contraction: input for biomechanical modelling and its validation. Biomech. Model. Mechanobiol. 12 (6), 1205–1220.

Borsdorf, M., Böl, M., Siebert, T., 2021. Influence of layer separation on the determination of stomach smooth muscle properties. Pflügers Arch. Eur. J. Physiol. 473 (6), 911–920.

Borsdorf, M., Tomalka, A., Stutzig, N., Morales-Orcajo, E., Böl, M., Siebert, T., 2019. Locational and directional dependencies of smooth muscle properties in pig urinary bladder. Front. Physiol. 10 (63), 1–12.

Bramich, N.J., Brading, A.F., 1996. Electrical properties of smooth muscle in the guinea-pig urinary bladder. J. Physiol. 492, 185–198.

Brown, A.L., Farhat, W., Merguerian, P.A., Wilson, G.J., Khoury, A.E., Woodhouse, K.A., 2002. 22 Week assessment of bladder acellular matrix as a bladder augmentation material in a porcine model. Biomaterials 23 (10), 2179–2190.

Cheng, F., Birder, L.A., Kullmann, F.A., Hornsby, J., Watton, P.N., Watkins, S., Thompson, M., Robertson, A.M., 2018. Layer-dependent role of collagen recruitment during loading of the rat bladder wall. Biomech. Model. Mechanobiol. 17 (2), 403–417.

Creed, K.E., Ishikawa, S., Ito, Y., 1983. Electrical and mechanical activity recorded from rabbit urinary bladder in response to nerve stimulation. J. Physiol. 338 (1), 149–164.

Dahms, S.E., Piechota, H.J., Dahiya, R., Lue, T.F., Tanagho, E.A., 1998. Composition and biomechanical properties of the bladder acellular matrix graft: comparative analysis in rat, pig and human. Br. J. Urol. 82 (3), 411–419.

Damaser, M.S., 1999. Whole bladder mechanics during filling. Scand. J. Urol. Nephrol. Suppl. 201, 51–58.

Drake, R., 2014. Gray's anatomy for students.

Durden, E., Walker, D., Gray, S., Fowler, R., Juneau, P., Gooch, K., 2018. The economic burden of overactive bladder (OAB) and its effects on the costs associated with other chronic, age-related comorbidities in the United States. Neurourol. Urodyn. 37 (5), 1641–1649.

Finkbeiner, A.E., O'Donnell, P.D., 1990. Responses of detrusor smooth muscle to stretch and relaxation: In vitro study. Urology 36 (2), 193–198.

FitzGerald, M.P., Stablein, U., Brubaker, L., 2002. Urinary habits among asymptomatic women. Am. J. Obstet. Gynecol. 187 (5), 1384–1388.

Gakhar, G., Wight-Carter, M., Andrews, G., Olson, S., Nguyen, T.A., 2009. Hydronephrosis and urine retention in estrogen-implanted athymic nude mice. Vet. Pathol. 46 (3), 505–508.

Gilbert, T.W., Wognum, S., Joyce, E.M., Freytes, D.O., Sacks, M.S., Badylak, S.F., 2008. Collagen fiber alignment and biaxial mechanical behavior of porcine urinary bladder derived extracellular matrix. Biomaterials 29 (36), 4775–4782.

Gloeckner, D.C., Sacks, M.S., Fraser, M.O., Somogyi, G.T., de Groat, W.C., Chancellor, M.B., 2002. Passive biaxial mechanical properties of the rat bladder wall after spinal cord injury. J. Urol. 167 (5), 2247–2252.

Gray, T., Phillips, L., Li, W., Buchanan, C., Campbell, P., Farkas, A., Abdi, S., Radley, S., 2019. Evaluation of bladder shape using transabdominal ultrasound: Feasibility of a novel approach for the detection of involuntary detrusor contractions. Ultrasound 27 (3), 167–175.

Griffiths, D.J., van Mastrigt, R., van Duyl, W.A., Coolsaet, B.L.R.A., 1979. Active mechanical properties of the smooth muscle of the urinary bladder. Med. Biol. Eng. Comput. 17 (3), 281–290.

Gunst, S.J., 1986. Effect of length history on contractile behavior of canine tracheal smooth muscle. Am. J. Physiol. Cell Physiol. 250 (1), C146–C154.

Heppner, T.J., Tykocki, N.R., Hill-Eubanks, D., Nelson, M.T., 2016. Transient contractions of urinary bladder smooth muscle are drivers of afferent nerve activity during filling. J. Gen. Physiol. 147 (4), 323–335.

Jorgensen, T.M., Djurhuus, J.C., Jørgensen, H.S., Sørensen, S.S., 1983. Experimental bladder hyperreflexia in pigs. Urol. Res. 11 (5), 239–240.

Kanai, A., Andersson, K.E., 2010. Bladder afferent signaling: Recent findings. J. Urol. 183 (4), 1288–1295.

Kaplan, S.A., Blaivas, J.G., Brown, W.C., Levin, R.M., 1991. Parameters of detrusor contractility: I: The effects of electrical stimulation, hysteresis, and bladder volume in an in vitro whole rabbit bladder model. Neurourol. Urodyn. 10 (1), 53–59.

Kim, A.K., Hill, W.G., 2017. Effect of filling rate on cystometric parameters in young and middle aged mice. Bladder 4 (1).

Koo, H.P., Macarak, E.J., Zderic, S.A., Duckett, J.W., 3rd Synder, H.M., Levin, R.M., 1995. The ontogeny of bladder function in the fetal calf. J. Urol. 154 (1), 283–287.

Korossis, S., Bolland, F., Ingham, E., Fisher, J., Kearney, J., Southgate, J., 2006. Review: Tissue engineering of the urinary bladder: Considering structure-function relationships and the role of mechanotransduction. Tissue Eng. 12 (4), 635–644.

Korossis, S., Bolland, F., Southgate, J., Ingham, E., Fisher, J., 2009. Regional biomechanical and histological characterisation of the passive porcine urinary bladder: Implications for augmentation and tissue engineering strategies. Biomaterials 30 (2), 266–275.

Latini, J.M., Mueller, E., Lux, M.M., FitzGerald, M.P., Kreder, K.J., 2004. Voiding frequency in a sample of asymptomatic American men. J. Urol. 172 (3), 980–984.

Lee, T., Yoon, S.M., 2013. The role of intra-abdominal pressure measurement in awake rat cystometry. Int. Neurourol. J. 17 (2), 44–47.

Lentle, R.G., Reynolds, G.W., Janssen, P.W.M., Hulls, C.M., King, Q.M., Chambers, J.P., 2015. Characterisation of the contractile dynamics of the resting ex vivo urinary bladder of the pig. BJU Int. 116 (6), 973–983.

Longhurst, P.A., Wein, A.J., Levin, R.M., 1991. In vitro models of bladder contraction and function. Neurourol. Urodyn. 10 (1), 97–109.

Lu, S.H., Sacks, M.S., Chung, S.Y., Gloeckner, D.C., Pruchnic, R., Huard, J., de Groat, W.C., Chancellor, M.B., 2005. Biaxial mechanical properties of muscle-derived cell seeded small intestinal submucosa for bladder wall reconstitution. Biomaterials 26 (4), 443–449.

Martins, P.A.L.S., Filho, A.L.S., Fonseca, A.M.R.M., Santos, A., Santos, L., Mascarenhas, T., Jorge, R.M.N., Ferreira, A.J.M., 2011. Uniaxial mechanical behavior of the human female bladder. Int. Urogynecol. J. 22 (8), 991–995.

Matsumoto, S., Chichester, P., Bratslavsky, G., Kogan, B.A., Levin, R.M., 2002. The functional and structural response to distention of the rabbit whole bladder in vitro. J. Urol. 168 (6), 2677–2681.

Menzel, R., Böl, M., Siebert, T., 2017. Importance of contraction history on muscle force of porcine urinary bladder smooth muscle. Int. Urol. Nephrol. 49 (2), 205–214.

Mevcha, A., Drake, M., 2010. Etiology and management of urinary retention in women. Indian J. Urol. 26 (2), 230–235.

Mills, I.W., Drake, M.J., Greenland, J.E., Noble, J.G., Brading, A.F., 2000a. The contribution of cholinergic detrusor excitation in a pig model of bladder hypocompliance. BJU Int. 86 (4), 538–543.

Mills, I.W., Noble, J.G., Brading, A.F., 2000b. Radiotelemetered cystometry in pigs: validation and comparison of natural filling versus diuresis cystometry. J. Urol. 164 (5), 1745–1750.

Morales-Orcajo, E., Siebert, T., Böl, M., 2018. Location-dependent correlation between tissue structure and the mechanical behaviour of the urinary bladder. Acta Biomater. 75, 263–278.

Murphy, R.A., 2011. Mechanics of vascular smooth muscle. Compr. Physiol. 325–351.

Murtada, S.C., Arner, A., Holzapfel, G.A., 2012. Experiments and mechanochemical modeling of smooth muscle contraction: Significance of filament overlap. J. Theoret. Biol. 297, 176–186.

Nagatomi, J., Gloeckner, D.C., Chancellor, M.B., de Groat, W.C., Sacks, M.S., 2004. Changes in the biaxial viscoelastic response of the urinary bladder following spinal cord injury. Ann. Biomed. Eng. 32 (10), 1409–1419.

Nagatomi, J., Toosi, K.K., Chancellor, M.B., Sacks, M.S., 2008. Contribution of the extracellular matrix to the viscoelastic behavior of the urinary bladder wall. Biomech. Model. Mechanobiol. 7 (5), 395–404.

Natali, A.N., Audenino, A.L., Artibani, W., Fontanella, C.G., Carniel, E.L., Zanetti, E.M., 2015. Bladder tissue biomechanical behavior: Experimental tests and constitutive formulation. J. Biomech. 48 (12), 3088–3096.

Nenadic, I.Z., Qiang, B., Urban, M.W., de Araujo Vasconcelo, L.H., Nabavizadeh, A., Alizad, A., Greenleaf, J.F., Fatemi, M., 2013. Ultrasound bladder vibrometry method for measuring viscoelasticity of the bladder wall. Phys. Med. Biol. 58 (8), 2675–2695.

Parekh, A., Cigan, A.D., Wognum, S., Heise, R.L., Chancellor, M.B., Sacks, M.S., 2010. Ex vivo deformations of the urinary bladder wall during whole bladder filling: Contributions of extracellular matrix and smooth muscle. J. Biomech. 43 (9), 1708–1716.

Parsons, B.A., Drake, M.J., Gammie, A., Fry, C.H., Vahabi, B., 2012. The validation of a functional, isolated bladder model from a large animal. Front. Pharmacol. 3, 52.

Philyppov, I.B., Sotkis, G.V., Rock, A., Roudbaraki, M., Bonnal, J.L., Mauroy, B., Prevarskaya, N., Shuba, Y.M., 2020. Alterations in detrusor contractility in rat model of bladder cancer. Sci. Rep. 10 (1), 19651.

Pratusevich, V.R., Seow, C.Y., Ford, L.E., 1995. Plasticity in canine airway smooth muscle. J. General Physiol. 105 (1), 73–94.

Ratz, Paul H., Speich, John E., 2010. Evidence that actomyosin cross bridges contribute to passive tension in detrusor smooth muscle. Amer. J. Physiol. Renal Physiol. 298 (6), F1424–F1435.

Rocha, J.N., 2017. Cystometric analysis of the transplanted bladder. Int. Braz. J. Urol. 43 (1), 112–120.
Rohrmann, D., Zderic, S.A., Duckett, Jr., J.W., Levin, R.M., Damaser, M.S., 1997. Compliance of the obstructed fetal rabbit bladder. Neurourol. Urodyn. 16 (3), 179–189.
Seow, C.Y., 2005. Myosin filament assembly in an ever-changing myofilament lattice of smooth muscle. Am. J. Physiol. Cell Physiol. 289 (6), C1363–C1368.
Seow, C.Y., Pratusevich, V.R., Ford, L.E., 2000. Series-to-parallel transition in the filament lattice of airway smooth muscle. J. Appl. Physiol. 89 (3), 869–876.
Seydewitz, R., Menzel, R., Siebert, T., Böl, M., 2017. Three-dimensional mechano-electrochemical model for smooth muscle contraction of the urinary bladder. J. Mech. Behav. Biomed. Mater. 75, 128–146.
Siebert, T., Leichsenring, K., Rode, C., Wick, C., Stutzig, N., Schubert, H., Blickhan, R., Böl, M., 2015. Three-dimensional muscle architecture and comprehensive dynamic properties of rabbit gastrocnemius, plantaris and soleus: Input for simulation studies. PLoS One 10 (6), e0130985.
Speich, J.E., Almasri, A.M., Bhatia, H., Klausner, A.P., Ratz, P.H., 2009. Adaptation of the length-active tension relationship in rabbit detrusor. Amer. J. Physiol. Renal Physiol. 297 (4), F1119–F1128.
Speich, J.E., Dosier, C., Borgsmiller, L., Quintero, K., Koo, H.P., Ratz, P.H., 2007. Adjustable passive length-tension curve in rabbit detrusor smooth muscle. J. Appl. Physiol. 102 (5), 1746–1755.
Stålhand, J., Holzapfel, G.A., 2016. Length adaptation of smooth muscle contractile filaments in response to sustained activation. J. Theoret. Biol. 397, 13–21.
Takezawa, K., Kondo, M., Kiuchi, H., Soda, T., Takao, T., Miyagawa, Y., Tsujimura, A., Nonomura, N., Shimada, S., 2014. Combination of bladder ultrasonography and novel cystometry method in mice reveals rapid decrease in bladder capacity and compliance in LPS-induced cystitis. Amer. J. Physiol. Renal Physiol. 307 (2), F234–F241.
Tomalka, A., Borsdorf, M., Böl, M., Siebert, T., 2017. Porcine stomach smooth muscle force depends on history-effects. Front. Physiol. 8, 802.
Toosi, K.K., Nagatomi, J., Chancellor, M.B., Sacks, M.S., 2008. The effects of long-term spinal cord injury on mechanical properties of the rat urinary bladder. Ann. Biomed. Eng. 36 (9), 1470–1480.
Toppercer, A., Tetreault, J.P., 1979. Compliance of the bladder: An attempt to establish normal values. Urology 14 (2), 204–205.
Trostorf, R., Morales-Orcajo, E., Siebert, T., Böl, M., 2021. Location- and layer-dependent biomechanical and microstructural characterisation of the porcine urinary bladder wall. J. Mech. Behav. Biomed. Mater. 115, 104275.
Tuna, B.G., Bakker, E.N.T.P., Van Bavel, E., 2012. Smooth muscle biomechanics and plasticity: relevance for vascular calibre and remodelling. Basic Clin. Pharmacol. Toxicol. 110 (1), 35–41.
Turner, A.M., Subramaniam, R., Thomas, D.F.M., Southgate, J., 2008. Generation of a functional, differentiated porcine urothelial tissue in vitro. Eur. Urol. 54 (6), 1423–1432.
Uvelius, B., 1976. Isometric and isotonic length-tension relations and variaitonsin cell length in longitudinal smooth muscel from rabbit urinary bladder. Acta Physiol. Scand. 97 (1), 1–12.
Uvelius, B., 1979. Shortening velocity, active force and homogeneity of contraction during electrically evoked twitches in smooth muscle from rabbit urinary bladder. Acta Physiol. Scand. 106 (4), 481–486.
Uvelius, B., Gabella, G., 1980. Relation between cell length and force production in urinary bladder smooth muscle. Acta Physiol. Scand. 110 (4), 357–365.
van Asselt, E., Pel, J.J.M., Mastrigt, R., 2007. Shortening induced effects on force (re)development in pig urinary smooth muscle. J. Biomech. 40 (7), 1534–1540.
van Mastrigt, R., Glerum, J.J., 1985. Electrical stimulation of smooth muscle strips from the urinary bladder of the pig. J. Biomed. Eng. 7 (1), 2–8.
Wall, L.L., Wiskind, A.K., Taylor, P.A., 1994. Simple bladder filling with a cough stress test compared with subtracted cystometry for the diagnosis of urinary incontinence. Am. J. Obstet. Gynecol. 171 (6), 1472–1477.
Wang, C.C., Nagatomi, J., Toosi, K.K., Yoshimura, N., Hsieh, J.H., Chancellor, M.B., Sacks, M.S., 2009. Diabetes-induced alternations in biomechanical properties of urinary bladder wall in rats. Urology 73 (4), 911–915.
Yang, P.J., Pham, J., Choo, J., Hu, D.L., 2014. Duration of urination does not change with body size. Proc. Natl. Acad. Sci. 111 (33), 11932–11937.
Zanetti, E.M., Perrini, M., Bignardi, C., Audenino, A.L., 2012. Bladder tissue passive response to monotonic and cyclic loading. Biorheology 49 (1), 49–63.